International Journal of Environmental Science and Technology (2023) 20:10285–10296
https://doi.org/10.1007/s13762-022-04506-z

ORIGINAL PAPER

Synthesis of novel clay-based nanocomposite materials and its application in the remediation of arsenic contaminated water

R. Malsawmdawngzela[1] · Lalhmunsiama[2] · D. Tiwari[1] · S. Lee[3]

Received: 11 July 2021 / Revised: 11 July 2022 / Accepted: 26 August 2022 / Published online: 7 September 2022

Abstract

Arsenic is a toxic metalloid widely present in the aquatic environment, showing severe health hazards. Natural bentonite clay (BN) showed little affinity toward arsenic (arsenic(III) and arsenic(V)). However, organosilane functionalized clay showed greater affinity toward arsenic(III) and arsenic(V). Therefore, natural bentonite was functionalized with 3-mercaptopropyltrimethoxysilane (3-MPTS) and 3-aminopropyltrimethoxysilane (3-APTES). Materials' characterization was extensively conducted with advanced analytical methods and surface area analysis by the BET analyzer. Under batch experiments, the materials were then utilized to eliminate arsenic(III) and arsenic(V) in an aqueous medium. Compared to the pristine bentonite, the functionalized materials increased the adsorption capacities of arsenic(III) and arsenic(V). The moderate solution pH (pH 4–6) significantly favored the elimination of arsenic(III) and arsenic (V) by these advanced materials. The maximum sorption capacity of arsenic(III) by 3-MPTS/BN and arsenic (V) by 3-APTES/BN was found at 11.93 and 10.50 mg/g, respectively. These functionalized materials showed fast uptake of arsenic, which attained apparent equilibrium within 180 and 120 min of contact, respectively, for arsenic(III) and arsenic(V). The influence of ionic strength and several co-existing ions showed an insignificant influence on the removal effectiveness except in EDTA and phosphate. The results further showed the selectivity and efficiency of functionalized materials toward the studied pollutants. The novel functionalized materials showed potential for the efficient decontamination of arsenic.

Keywords Arsenic removal · Silane functionalized bentonite · Characterization of materials · Sorption mechanism · Adsorption isotherms · Kinetics of sorption

Introduction

The spreading of toxic arsenic in an aquatic environment is one of the world's most critical environmental issues. Human activities such as mining, pesticides, agriculture, etc., and natural processes, including volcanic eruption, and biological activity have led arsenic into the aquatic environment (Cortés-Arriagada and Toro-Labbé 2016; Song et al. 2017; Alka et al. 2021). Inorganic arsenic is relatively more toxic than organic arsenic and poses a severe threat to the environment (Sarkar and Paul 2016). The inorganic arsenic commonly exists as arsenite (As(III) and arsenate (As(V)) in the aquatic environment (Mohan and Pittman 2007; Luo et al. 2012). However, the toxicity and mobility of arsenic(III) are higher than arsenic(V) and complicated to eliminate from the aquatic environment (Zhu et al. 2016a; Maji et al. 2018). Generally, the intake of As by humans occurs through the consumption of contaminated water and food. Long-term exposure to high levels of As led to several biological disorders, such as skin lesions, inflammation in the kidney, blackfoot disease, cardiovascular disorders, diabetes, endocrine disorders, dysfunction of the respiratory system, hypertension, etc. (Sabir et al. 2019; Chen et al. 2019; Medda et al. 2021; Yadav et al. 2021). Moreover, inorganic arsenic is a Group 1 carcinogen (Wang et al. 2019). The WHO reduced the permissible quantity of arsenic in potable water

Editorial responsibility: Tanmoy Karak.

✉ D. Tiwari
diw_tiwari@yahoo.com

[1] Department of Chemistry, Mizoram University, Aizawl 796004, India

[2] Department of Industrial Chemistry, Mizoram University, Aizawl 796004, India

[3] Department of Health and Environmental, Catholic Kwandong University, Gangneung 210-701, Republic of Korea

to 10 µg/L (WHO 2011). Among Southeast Asian countries, people living in India, Bangladesh, China, Myanmar, Vietnam, Cambodia, Nepal, and Pakistan are significantly affected by arsenic (Uppal et al. 2019).

Different treatment processes, including chemical precipitation, oxidation, phytoremediation, coagulation-flocculation, adsorption, ion exchange, coagulation, membrane technologies, etc., are demonstrated to eliminate arsenic in water (Litter et al. 2019). However, the adsorption process is observed as a low-cost, efficient, and simple method for removing As from water bodies (Najib and Christodoulatos 2019; Kumar et al. 2019). Clay minerals are porous and extensively used to attenuate several contaminants from wastewaters. However, the hydrophilic nature of clay minerals makes it less favorable for the adsorption of anionic, non-polar species, and oxyanion species, viz., chromium, arsenic, etc. (Lee and Tiwari 2012). Bentonite is a montmorillonite-type clay that includes alumina and silicates with a molar ratio of 2:1. It carries a net negative charge on its surface. Therefore, the pristine bentonite showed less affinity to adsorb anionic species.

The chemical and physical properties make bentonite suitable adsorbents for several pollutants. The micro- and mesopores of bentonite are useful for the sorption of several sorbate species (Zhu et al. 2016b; Prabhu and Prabhu 2018; Chen et al. 2018). The surface modification of clay minerals using the suitable materials improve the applicability of clay in decontamination of wastewaters (Su et al. 2013; Gohain et al. 2020). Moreover, introducing the surfactant molecules, viz., hexamethylenediamine (HMDA), hexadecyltrimethylammonium bromide (HDTMA), etc. within the clay network nevertheless, are fairly good sorbing materials. However, these hybrid materials are having several drawbacks, including the formation of weaker bonds with clay, lower thermal stability, difficult to regenerate once loaded with pollutants (Sarkar et al. 2011; Wamba et al. 2018; Karki and Ingole 2022). Moreover, the loosely bound surfactant molecule readily release in aqueous medium and contaminating the waterbodies. However, on the other hand the silylation/grafting of clay minerals using suitable organo-functional groups (amine or thiol) has attracted attention. The material is synthesized by a strong covalent bond between clay and organic group, which results in enhanced stability of materials.

The silylation occurs at the internal and external surfaces of clay minerals under moderate circumstances. It was observed that the property and structure of the grafted products strongly depend on the reaction conditions (He et al. 2013; Karki et al. 2021). Therefore, this study aims to functionalize the pristine bentonite with different silanes, viz., 3-mercaptopropyltrimethoxysilane and 3-aminopropyltriethoxysilane. Further, the functionalized materials were used to treat water polluted with arsenic(III) and arsenic(V) under batch studies. The efficiency of the functionalized solids for arsenic(III) and arsenic(V) was obtained. Moreover, the parametric studies, viz., the effect of solution pH, contact time, pollutant concentrations, and ionic strength, are extensively studied to demonstrate the uptake mechanism of arsenic by these novel functionalized materials.

Materials and methods

Included as supplementary material D1.

Methodology

Functionalization of bentonite clay

The pristine bentonite was functionalized with organosilane in a facile one-pot process. Bentonite powder (12 g) was taken in toluene (300 mL) in a round bottom flask. The mixture was refluxed for 30 min at 60 °C in an N_2 environment. 3-mercaptopropyletrimethoxy (12 mL) was slowly mixed. The solution mixture was refluxed overnight. The slurry was then rinsed with toluene, followed by ethanol. The solid powder was dried at 100 °C. The process enabled the grafting of 3-mercaptopropyletrimethoxy with bentonite and assigned as 3-MPTS/BN. The similar process was followed to functionalize the bentonite using 3-aminopropyltriehoxysilane, and is named 3-APTES/BN. The experiments were performed to obtain the point of zero charges (pH_{PZC}) of raw bentonite, 3-MPTS/BN, and 3-APTES/BN following the method described previously (Lalhmunsiama et al. 2013).

Characterization

Included as supplementary material D2.

Sorption studies

Different studies were performed to study the effect of pH, contact time, co- ions, ionic strength, and initial arsenic(III)/or arsenic(V) concentrations under batch studies. Batch results demonstrated the sorption reaction mechanisms at the solid/solution interface. 50.0 mL of arsenic(III)/or arsenic(V) solution was kept in the airtight containers, the

solution pH was maintained between pH values (2.0 to 10.0) and 0.1 g of raw bentonite or 3-MPTS/BN or 3-APTES/BN material was introduced into each container. The containers were put in an automatic shaker for 24 h at 25 ± 2 °C. The containers were taken out from the shaker, the suspensions were filtered with 0.45 µm filter paper. The solution pH was rechecked and taken as the final pH. The atomic absorption spectrometer (AAS) analyzed for the arsenic in the treated water samples. The initial concentration (arsenic(III)/arsenic(V)) effect was performed at concentrations between 1.0 to 25.0 mg/L at pH 3.5 using the functionalized materials. The time-dependent study was conducted between 5 to 720 min on the sorption of arsenic(III)/arsenic(V) at pH 3.5 with initial arsenic(III)/arsenic(V) concentration of 10 mg/L at 25 ± 2 °C. The impact of ionic strength (0.0001 to 0.1 mol/L NaCl at pH 3.5) on the removal of arsenic(III)/arsenic(V) was performed at 25 ± 2 °C. The removal of arsenic is assessed in the presence of different co-anions (EDTA, glycine, oxalic acid, and phosphate) and co-cations (magnesium(II), manganese(II), nickel(II), calcium(II)). The concentration of each co-ion was taken 50.0 mg/L and arsenic (III)/arsenic(V) 10.0 mg/L at constant pH 3.5.

Results and discussions

Materials characterization

The FT-IR results envisage the functional groups present with materials, and the results are shown in Fig. 1a. The FT-IR spectra of 3-MPTS/BN showed weak vibrational bands at 2927 and 2858 cm^{-1} assigned to the C–H stretching vibrations (Tonlé et al. 2007; Su et al. 2011). A noticeable vibrational band at 2914 cm^{-1} was assigned to the presence of methoxy group (–OCH_3) from 3-MPTS (Yılmaz et al. 2017; Şahan et al. 2018). The thiol (–SH) group from 3-MPTS was observed at stretching vibration around 2550 cm^{-1} (Tonlé et al. 2008). The small distinguishable peaks at 690 and 1410 cm^{-1} were assigned as C–H and C–S deformation and stretching vibrations of thiol groups (3-MPTS/BN solids) (Carvalho et al. 2008). Moreover, the 3-APTES/BN graph displayed a tiny band at 1490 cm^{-1} due to the bending vibration of aliphatic CH_2 (Undabeytia et al. 2019). A weak peak at ~ 1319 cm^{-1} indicates the C–N stretching vibration of grafted silane with the bentonite (Asgari et al. 2017). Moreover, a small distinct band at 2970 cm^{-1} was due to the symmetric stretching vibrations of the methylene group of organosilane (Mostofi Sarkari et al. 2019).

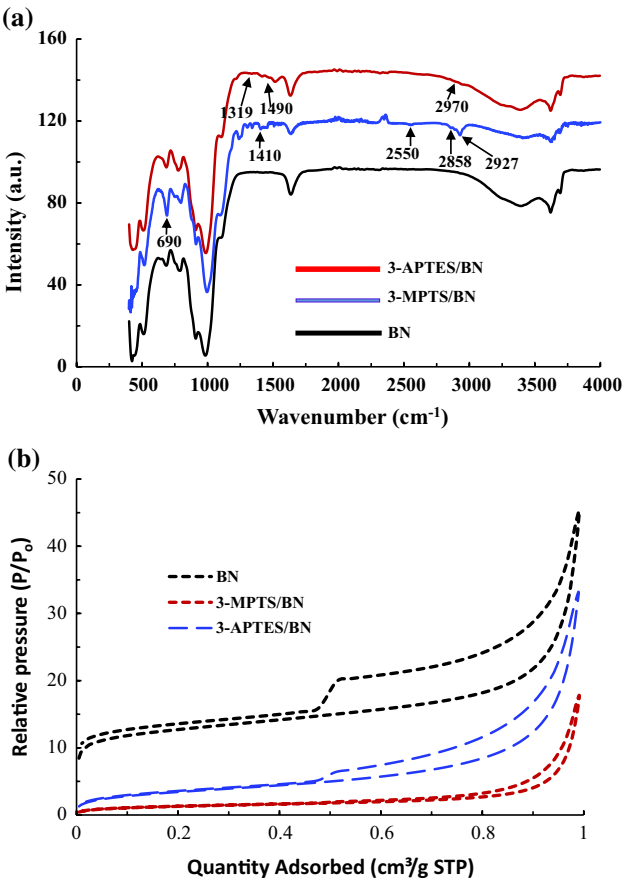

Fig. 1 **a** FT-IR graph; and **b** N_2 adsorption–desorption isotherms for BN, 3-MPTS/BN, and 3-APTES/BN solids

The textural properties of raw bentonite and functionalized materials were evaluated from the N_2 adsorption–desorption isotherms obtained by BET method. It is evident from Fig. 1b that these solids had the type IV isotherm having H3 hysteresis. Results inferred that the bare clay and the functionalized materials were contained with mesopores (Paul et al. 2011; Qin et al. 2014). Figure 1b reveals a bigger hysteresis loop for raw bentonite with pore size and pore volume of 68.42 Å and 0.078 cm^3/g, respectively. The pore size and pore volume of 3-MPTS/BN and 3-APTES/BN were 68.37 Å, 0.071 cm^3/g, and 165.11 Å, 0.052 cm^3/g, respectively. The specific surface area of bentonite, 3-MPTS/BN, and 3-APTES/BN were 41.11, 4.68, and 12.51 m^2/g, respectively. The specific surface area of 3-MPTS/BN and 3-APTES/BN is considerably smaller than the pristine bentonite. The pores on the clay surface were incorporated with the 3-MPTS/3-APTES molecules hence, caused for reduced surface area. Previously, it was reported that hybrid material

Table 1 X-ray diffraction peaks of bare bentonite (BN), 3-MPTS/BN, and 3-APTES/BN

BN			3-MPTS/BN			3- APTES/BN		
Peak position (2 theta)	d-spacings [Å]	Relative Intensity	Peak position (2 theta)	d-spacings [Å]	Relative Intensity	Peak position (2 theta)	d-spacings [Å]	Intensity
6.3001	14.0296	17.63	6.8127	12.975	15.19	7.8236	11.3006	2.32
9.6366	9.17825	7.64	9.6833	9.13404	8.63	–	–	–
12.4995	7.08174	8.48	12.2167	7.24501	6.94	11.9105	7.4306	4.38
19.845	4.47397	38.12	19.5763	4.53477	47.58	19.5714	4.53589	34.44
20.9405	4.24053	35.24	20.7724	4.27627	41.55	20.538	4.32454	32.1
24.9889	3.56346	13.32	25.0495	3.55497	25.38	24.5224	3.63018	11.76
26.7726	3.32911	100	26.56	3.35614	100	26.3124	3.38715	100
28.021	3.18438	12.02	–	–	–	27.2693	3.27043	13
30.0445	2.97436	8.48	–	–	–	30.0418	2.97463	5.12
34.9046	2.57055	23.35	34.8343	2.57557	33.47	34.5382	2.59698	24.18
36.6733	2.44989	23.46	–	–	–	36.319	2.47362	17.85
39.5748	2.2773	8.51	41.9197	2.15518	3.3	39.1458	2.30126	8.46
45.5118	1.99309	2.79	–	–	–	42.1211	2.14534	10.84
50.2583	1.81508	16.09	50.015	1.82368	14.61	45.3991	1.99777	8.87
54.6967	1.67814	7.71	54.4257	1.68586	12.15	49.823	1.83026	17.85
61.0826	1.53995	12.23	–	–	–	54.838	1.67415	11.99
61.8523	1.50007	15.6	61.8119	1.50096	22.23	59.644	1.55022	12.9
68.3428	1.37223	9.7	67.9788	1.37904	5.96	61.4578	1.50875	21.47
73.3261	1.29112	5	73.1101	1.2944	6.77	67.8237	1.38181	12.72

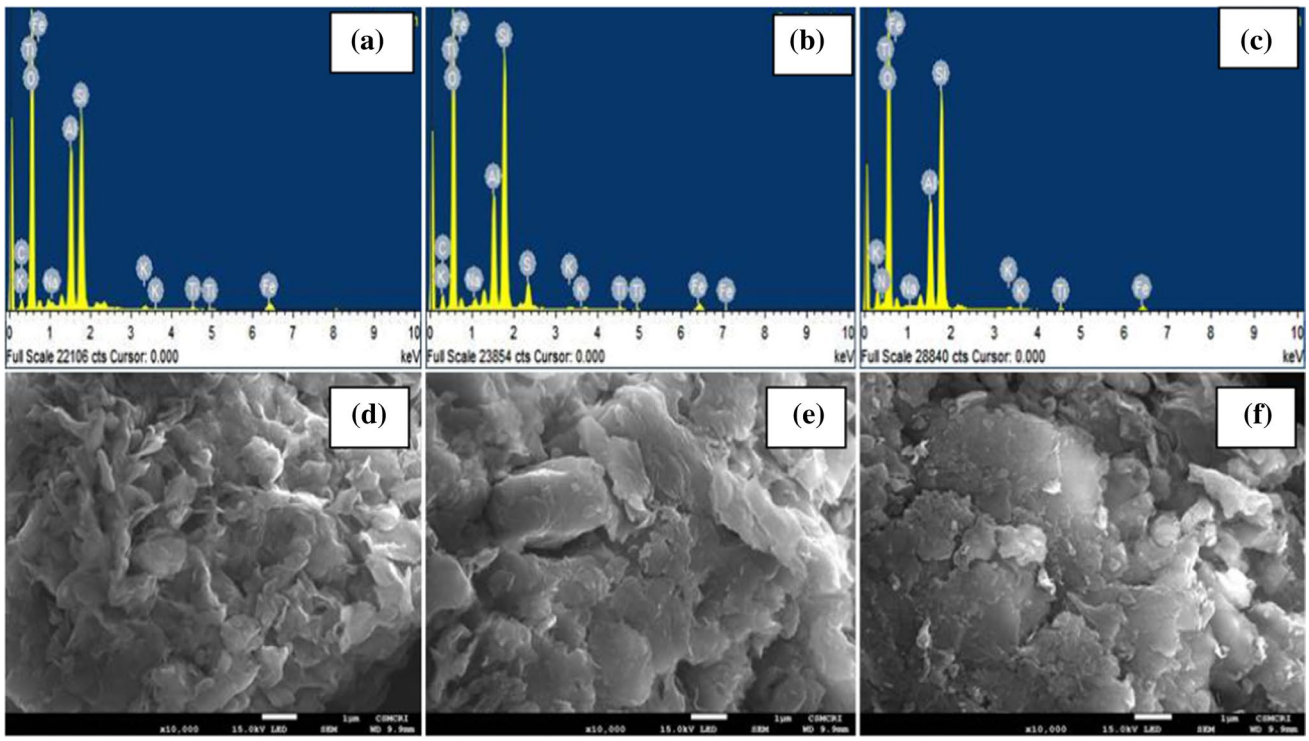

Fig. 2 EDX spectra of **a** raw bentonite; **b** 3-MPTS/BN; and **c** 3-APTES/BN and SEM images of **d** raw bentonite; **e** 3-MPTS/BN; and **f** 3-APTES/BN

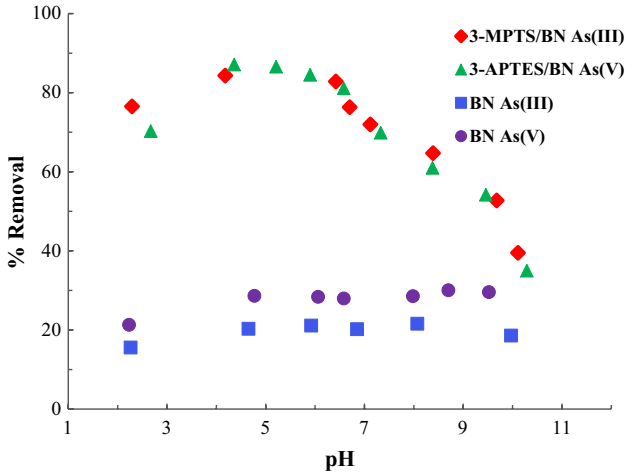

Fig. 3 pH-dependent removal of arsenic (III) and arsenic(V) by raw bentonite (BN), arsenic(III) using 3-MPTS/BN, and arsenic(V) using 3-APTES/BN

intercalated with surfactant molecules exhibited a drastic reduction in the specific surface area of the material (Tcheumi et al. 2010).

The solid samples BN, 3-MPTS/BN, and 3-APTES/BN were subjected to XRD analysis, and the data obtained are given in Table 1. XRD data showed that both the functionalized materials have almost identical crystalline structures compared to the bentonite. The diffraction peaks observed at two theta values of 20.94, 26.77, 36.67, 50.25, 61, and 68.34 indicating the presence of quartz a major constituent in all these three materials (Thanhmingliana and Tiwari 2015; Mohammed and Samaka 2018).

EDX analyses have been performed for the elemental composition of BN, 3-MPTS/BN, and 3-APTES/BN solids and shown in Fig. 2a, b, and c, respectively. Figure 2a, b, and c shows that all these solids are contained with the elements Si, Al, Ti, Fe, K, Na O, C, etc. These are the common components of the bentonite. However, on the other hand, Fig. 2b (the spectrum of 3-MPTS/BN) showed an additional peak of S which confirmed the grafting of 3-MPTS molecule within the bentonite. Similarly, the EDX spectrum of 3-APTES/BN showed an additional peak of N. This inferred that the solid is contained with the nitrogen containing compound, i.e., APTES is grafted with the bentonite. Further, the quantitative analysis showed that the carbon and nitrogen percentages were increased from 0.58 and 0.081% to 7.71 and 2.59%, respectively, once the clay is loaded with the 3-APTES.

The SEM micrographs of raw bentonite (BN), 3-MPTS/BN, and 3-APTES/BN are shown in Fig. 2d, f, and e, respectively. The SEM images obtained for 3-MPTS/BN and 3-APTES/BN showed disordered and messy surface structures. Furthermore, the figure clearly showed that the porosity of 3-MPTS/BN and 3-APTES/BN solids were significantly decreased compared to the unmodified clay which inferred that 3-MPTS/or 3-APTES molecules were incorporated inside the pores of the clay surface. The modification of natural attapulgite with organosilane (3-APTES) resulted in compact aggregate. At the same time, the unmodified clay showed a loose aggregate structure (Cui et al. 2013).

pH-Dependent sorption study

The pH-dependent elimination of arsenic(III) and arsenic(V) was performed between the solution pH 2.0–10.0 with arsenic(III) and arsenic(V) concentration 10.0 mg/L utilizing the raw bentonite (BN), 3-MPTS/BN, and 3-APTES/BN. The results are displayed in Fig. 3. The percentage elimination of raw bentonite was greatly enhanced after the functionalizion of materials. The removal of arsenic(III) and arsenic(V) by the solids 3-MPTS/BN and 3-APTES/BN, respectively, was considerably increased as compared to the raw bentonite. At around pH 7, the percentage uptake of arsenic(III) and arsenic(V) by the pristine bentonite was recorded ~ 30 and 20%, respectively. However, almost 90% of arsenic(III) and arsenic(V) were removed using the 3-MPTS/BN and 3-APTES/BN solids, respectively.

The speciation of the adsorbate, pH_{pzc}, and functional groups of adsorbents helps to demonstrate the solid/solution interface mechanism. The pH_{pzc} of the BN, 3-MPTS/BN, and 3-APTES/BN were obtained to be 7.81, 7.65, and 7.64, respectively. Therefore, below the pH_{pzc}, the materials have the net positive charge, and above pH_{pzc}, the materials have the net negative charge. On the other hand, the speciation of arsenic(III) and arsenic(V) revealed that arsenic(III) predominantly existed as neutral H_3AsO_3 species till pH 8.0 (Cf. Figure S1(a). Above this pH, the negatively charged oxyanion species $H_2AsO_3^-$ is dominant in the solution. In case of arsenic(V), a predominant neutral species (H_3AsO_4) occurred below pH 3.0. Further, increase in pH favored the acidic dissociation of (H_3AsO_4) and between pH 3.5–6.0, arsenic(V) existed in its oxyanion species ($H_2AsO_4^-$). Further, between pH 6.0–10.0, arsenic(V) existed to its dianionic species $HAsO_4^{2-}$ species (*Cf* Figure S1(b)). Therefore, arsenic(V) existed as anionic species of $H_2AsO_4^-$ or

$HAsO_4^{2-}$ in the studied pH range (pH ~ 3.0–10.0) (Tiwari and Lee 2012).

The sorption results indicated that the lower pH (~ pH 2.4–4.0) significantly suppressed the uptake of Arsenic(III) and arsenic(V) by the solids 3-MPTS/BN and 3-APTS/BN, respectively. A relatively lower uptake of arsenic(III) or arsenic(V) at lower pH region is due to the fact that the presence of excess of H^+ ions which competes and inhibited the attraction of arsenic species toward the solid surface. However, at higher pH (pH ~ 4.0–6.0), a significant enhanced uptake of arsenic(III) was attained due to the strong affinity of the surface functional groups with the arsenic(III) and possibly arsenic(III) forming the chelation with the thiol group of 3-MPTS/BN. Further, increase in pH > 6.41, a decrease in percentage elimination of arsenic(III) was observed. This is due to the acid dissociation of surface (pH_{pzc} of 3-MPTS/BN: 7.65), hence, the weakening of thiol-arsenic(III) bond resulted with lower uptake of arsenic by the 3-MPTS/BN solid. A similar results were demonstrated previously using the different materials thiol group containing materials (Hao et al. 2009; Li et al. 2014; Zhang et al. 2015).

On the other hand, a rapid increase in arsenic(V) removal efficiency by 3-APTES/BN was observed from pH 2.67 to 4.36 and remained constant until pH 6.58 and decreased significantly beyond pH 6.58. Enhanced uptake of arsenic(V) between pH 4.36 and 6.58 was due to anionic species $H_2AsO_4^-$ and the protonated amine group from 3-APTES. A stronger electrostatic attraction of arsenic(V) by the solid, resulted an enhanced uptake of arsenic(V). Further, the arsenic(V) is forming stronger chemical bond at the solid surface with the introduced amino group (Chen et al. 2009; Boyacı et al. 2011). The decline in the elimination of arsenic(V) by 3-APTES/BN above pH 6.57 was due to the strong electrostatic repulsion that operates between the negatively charged surface and the anionic species of arsenic(V), i.e., $H_2AsO_4^-$ and AsO_3^-. A similar results were reported previously for the sorption of arsenic(III) and arsenic(V) by the porous hybrid materials precursor to the bentonite (Lee et al. 2015).

Kinetic studies

The amount of arsenic(III) and arsenic(V) removed using the 3-MPTS/BN and 3-APTES/BN, respectively, were obtained at various contact times and shown in Fig. 4a. At first, the elimination of arsenic by these two functionalized materials was rapid and the arsenic(III) and arsenic(V) elimination exceeded 60% within 60 min. The removals of arsenic by

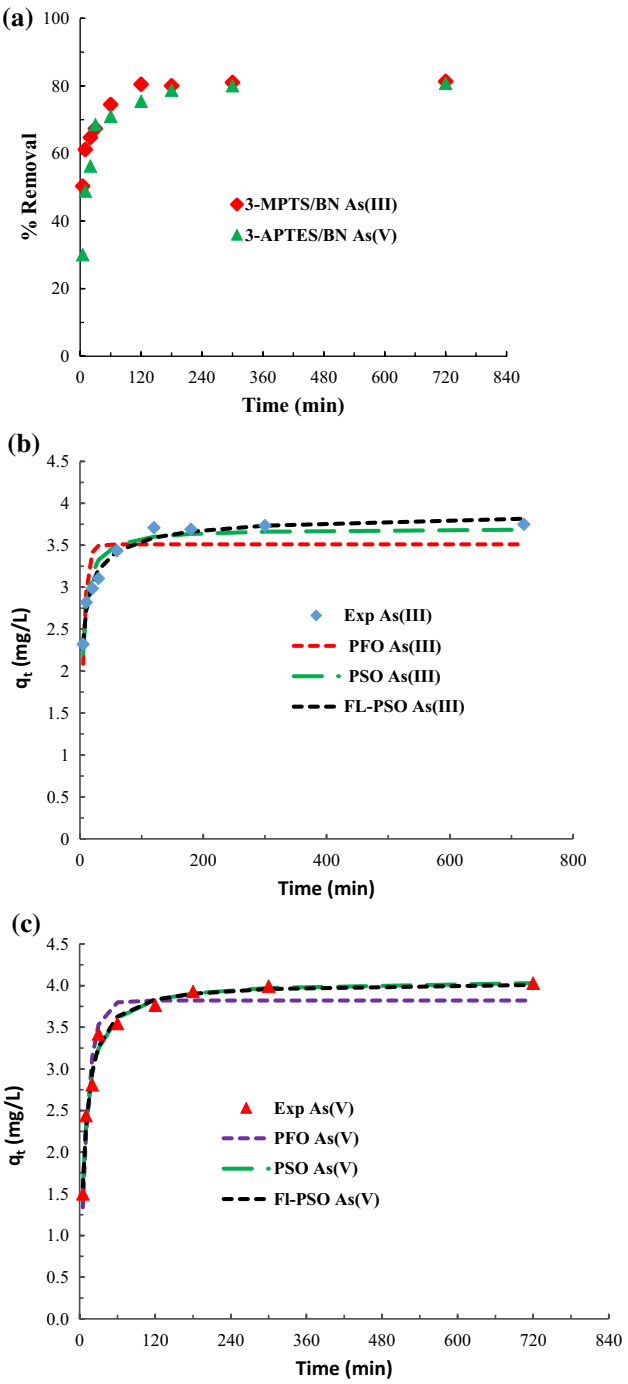

Fig. 4 **a** Time-dependent uptake of arsenic(III) by 3-MPTS/BN and arsenic(V) by 3-APTES/BN. The PFO, PSO, and FL-PSO kinetic models for the removal of **b** arsenic(III) by 3-MPTS/BN; and **c** arsenic(V) by 3-APTES/BN

Table 2 The rate constant obtained for PFO, PSO, and FL-PSO, models for removing arsenic(III) and arsenic(V) by functionalized materials

Material	Pollutants	PFO model			PSO model			FL–PSO model			
		q_e	k_1	s^2	q_e	k_2	s^2	q_e	k	α	s^2
3-MPTS/BN	Arsenic(III)	3.511	0.18	0.59	3.703	0.078	0.127	3.939	0.137	0.614	0.044
3-APTES/BN	Arsenic(V)	3.821	0.086	0.355	4.074	0.161	0.088	4.041	0.028	1.057	0.085

these materials were rapid during the initial period since many active sites on the adsorbent are readily accessible for sorbate species. The rate of arsenic removal was reduced with time and reached equilibrium at 120 and 180 min for arsenic(III) using 3-MPTS/BN and arsenic(V) using 3-APTES/BN solids. This finding inferred the suitability of the synthesized functionalized materials in treating water polluted with arsenic.

The adsorption data at different contact times for the elimination of arsenic(III) by 3-MPTS/BN and arsenic(V) by 3-APTES/BN were employed to plot the three non-linear kinetic models, viz., pseudo-first-order (PFO), pseudo-second-order (PSO) and fractal-like pseudo-second-order (FL-PSO) models using the known equations (Thanhmingliana and Tiwari 2015). Figures 4b and c shows the fitting results. The least-square sum and other constants are given in Table 2. The figure and calculated data show that the time-dependent adsorption data are well fitted to the PSO and FL-PSO models than the PFO model since the least square sum was found reasonably low for the PSO and FL-PSO models. These results further indicated that arsenic(III) and arsenic(V) forming stronger chemical bonds at the solid surface.

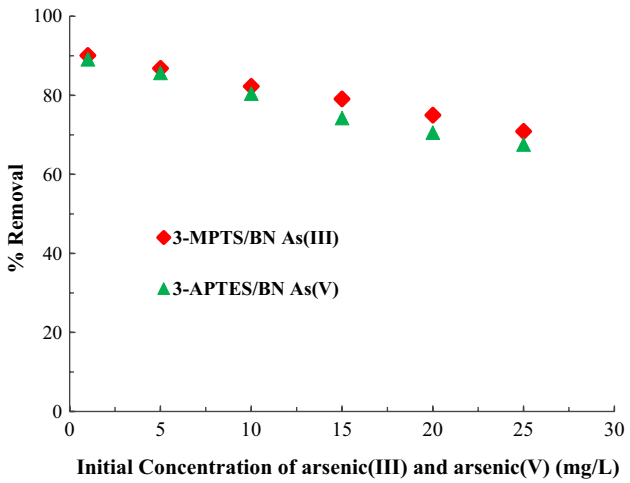

Fig. 5 Percentage elimination of arsenic(III) and arsenic(V) using solids at different initial concentrations

Concentration-dependent study

The concentration-dependent elimination of arsenic(III) and arsenic(V) were conducted, varying the initial concentrations of arsenic between 1.0 to 25.0 mg/L utilizing the 3-MPTS/BN and 3-APTES/BN at a solid dose of 2.0 g/L, and the percentage elimination at different concentrations are shown in Fig. 5. Increasing the concentration of arsenic from 1.0 to 25.0 mg/L caused for decrease in percentage elimination of arsenic from 89 to 67% (for arsenic(V) by 3-APTES/BN) and 90% to 70% (for arsenic(III) by 3-MPTS/BN). Relatively very high uptake of arsenic by these solids even at higher sorbate concentrations indicated that arsenic(III) and arsenic(V) showed high affinity toward the functionalized materials.

The Langmuir, Freundlich, and Temkin adsorption isotherms were employed to deduce the sorption isotherms using the sorptive concentration-dependent sorption data (Lalhmunsiama et al. 2015; Vahedi et al. 2018;), and the graphs are shown in Figure S2(a, b and c). The unknown parameters, i.e., Langmuir monolayer sorption capacity (q_o), Langmuir constant (b), Freundlich constants (K_f and $1/n$), and Temkin constants, A (L/g) and B (J/mol), were calculated and given in Table 3. The linear fitting of data indicated that the Langmuir and Freundlich adsorption isotherms are more favorable than the Temkin isotherm since the higher value of R^2 was obtained for these isotherms. The applicability of the Langmuir isotherm indicated that the sorbate species are forming the monolayer coverage and the surface-active sites are homogeneously distributed. Moreover, the sorbate species are forming the stronger chemical bond on the surface which also confirmed with the applicability of the Freundlich adsorption isotherm. Moreover, the Freundlich isotherm hypothesized that the surface-active sites are heterogeneously distributed (Kecili and Hussain, 2018). The Langmuir sorption capacity obtained removing arsenic(V) by 3-APTES/BN and arsenic(III) using 3-MPTS/BN were 10.50 and

Table 3 Langmuir, Freundlich, and Temkin constants obtained for the sorption of arsenic(V) and arsenic(III)

Material	Pollutants	Langmuir			Freundlich			Temkin		
		q_o (mg/g)	b (L/g)	R^2	$1/n$	K_f (mg/g)	R^2	B (J/mol)	A (L/g)	R^2
3-APTES/BN	Arsenic(V)	10.504	0.594	0.99	0.672	2.257	0.987	4.101	2.374	0.922
3-MPTS/BN	Arsenic(III)	11.933	0.535	0.995	0.668	2.254	0.993	4.06	2.387	0.922

11.93 mg/g, respectively. Table 3 shows moderately higher values of Langmuir constant (b) and Freundlich constant (K_F), and Temkin constants A (L/g) and B (J/mol) reaffirmed the high affinity of the functionalized materials to the arsenic(V) and arsenic(III) in aqueous media. Further, the positive value of B (J/mol) indicated that the sorption process involved an 'exothermic reaction'.

Impact of ionic strength

The efficiency of the functionalized materials for arsenic(III) and arsenic(V) at various ionic strengths was evaluated. Figure 6 shows the effect of 1000 times rise in NaCl concentration eliminating arsenic(III) and arsenic(V) by functionalized materials, and the percentage removal remains almost unchanged. These findings inferred that arsenic(III) and arsenic(V) formed the inner-sphere complexes onto the functionalized materials hence, aggregated with relatively strong chemical forces. These results further supported the pH dependence and adsorption isotherm

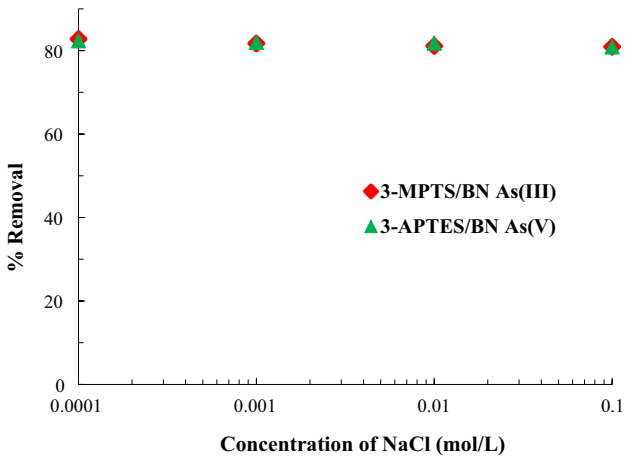

Fig. 6 Effect of various concentrations of sodium chloride in the elimination of arsenic(III) and arsenic(V) by the functionalized materials

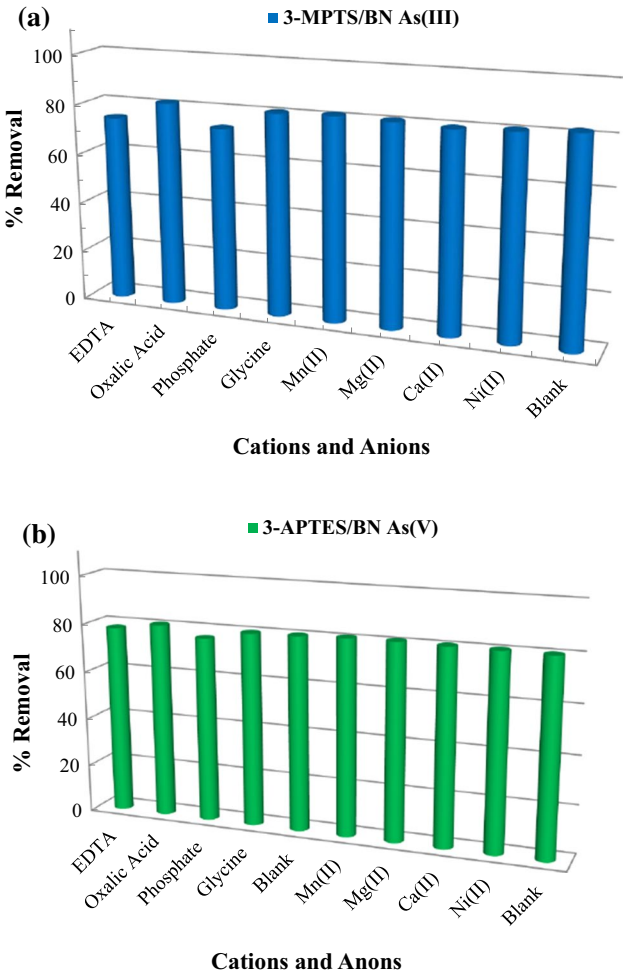

Fig. 7 Percentage elimination of **a** arsenic(III) by 3-MPTS/BN and **b** arsenic(V) by 3-APTES/BN materials in the presence of co-ions (cation and anions)

results presented previously. The variation of ionic strengths readily influences the outer-sphere complex at the solid surface, while the inner-sphere complex is unaffected by an increase in ionic strength (Li et al. 2019). Similar influences of ionic strength were obtained in the elimination of arsenic(III) and arsenic(V) using manganese and iron pillared clay (Mishra and Mahato 2016). Moreover, the presence of Ca^{2+}, Mg^{2+}, Cl^{-}, $SO^{2-}{}_4$, and $CO_3{}^{2-}$ did not display substantial influence in the elimination of arsenic(III) and arsenic(V) using molybdate impregnated chitosan beads (Chen et al. 2008).

Presence of co-ions

The elimination of arsenic (III) and arsenic(V) in the existence of several ions were studied with the initial arsenic(III)/arsenic(V) and co-ions concentration of 10.0 and 50.0 mg/L, respectively. The cations were taken as manganese(II), magnesium(II), calcium(II), and nickel(II). In contrast, the anions were selected ethylenediaminetetraacetic acid, glycine, phosphate, and oxalic acid. Figures 7a and b shows the effect of cations and anions on the elimination efficiency of arsenic(III) and arsenic(V) by these functionalized materials. Arsenic(III) elimination by 3-MPTS/BN was reduced from 82 to 74% and 82 to 73% in the presence of EDTA and $PO_4{}^{3-}$, respectively. Similarly, the percent removal of arsenic(V) by 3-APTES/BN was decreased by 80 to 78% and 80 to 76% in the presence of EDTA and phosphate, respectively. Previously it was reported that anions, $HCO_3{}^{-}$, and $SO_4{}^{2-}$ did not influence the sorption efficiency of arsenic(V) onto Fe-modified charred granulated attapulgite. A slight reduction, i.e., 4.60% and 1.10% in the presence of $HCO_3{}^{-}$ and $SO_4{}^{2-}$, respectively, was observed. On the other hand, the presence of $PO_4{}^{3-}$ considerably reduced the arsenic(V) removal using the same material and showed a maximum effect on the elimination of arsenic(III). Due to similar chemical properties of phosphate and arsenic, $PO_4{}^{3-}$ and arsenic compete toward the same active sites in Fe-modified charred granulated attapulgite hence, caused for more significant impact in the removal of arsenic (Yin et al. 2017). Several researchers previously reported similar results (Gong et al. 2015; Ociński et al. 2016; Te et al. 2017). Maji et al. observed that Ca^{2+} and Fe^{2+} in the aqueous media showed an insignificant effect on the uptake amount of As by laterite soil (Maji et al. 2007).

Conclusion

Bentonite clay was functionalized by the mercapto/amino groups using organosilanes viz., 3-mercaptopropyltrimethoxysilane and 3-aminopropyltriethoxysilane, respectively. The FT-IR and the EDX analyses proved the successful silylation of bentonite. The silanes were aggregated within the pores of bentonite and grafted with a strong chemical bond. The mercapto and amino-functionalized bentonite show enhanced elimination of arsenic(III) and arsenic(V) within the pH 4.0–6.0. A strong affinity of arsenic(III) toward the 3-MPTS/BN and arsenic(V) toward the 3-APTS/BN was observed and the arsenic species were aggregated with stronger chemical forces at the respective solid surface. The kinetic data show that the PSO and EL-PSO models are more favorable than the PFO kinetic model. The Langmuir and Freundlich adsorption models described the sorption of arsenic(III) and arsenic(V) by the functionalized materials. The Langmuir sorption capacity was 11.93 mg/g and 10.50 for arsenic(III) by 3-MPTS/BN and for arsenic(V) by 3-APTES/BN solids, respectively. One thousand times increase in ionic strength did not affect the sorption of arsenic onto the functionalized materials. However, EDTA and phosphate in solution affected the removal efficiency of functionalized materials for arsenic(III) or arsenic(V). Results inferred that the functionalized materials possessed an enhanced selectivity and applicability toward arsenic in the aqueous medium. Hence, it is found to be efficient and potential in the possible implications for decontaminating the arsenic-contaminated water.

Supplementary Information The online version contains supplementary material available at https://doi.org/10.1007/s13762-022-04506-z.

Acknowledgments The authors wish to thank all who assisted in conducting this work.

References

Alka S, Shahir S, Ibrahim N et al (2021) Arsenic removal technologies and future trends: a mini review. J Clean Prod 278:123805. https://doi.org/10.1016/j.jclepro.2020.123805

Asgari M, Abouelmagd A, Sundararaj U (2017) Silane functionalization of sodium montmorillonite nanoclay and its effect on rheological and mechanical properties of HDPE/clay nanocomposites. Appl Clay Sci 146:439–448. https://doi.org/10.1016/j.clay.2017.06.035

Boyacı E, Çağır A, Shahwan T, Eroğlu AE (2011) Synthesis, characterization and application of a novel mercapto- and amine-bifunctionalized silica for speciation/sorption of inorganic arsenic prior to inductively coupled plasma mass spectrometric determination. Talanta 85:1517–1525. https://doi.org/10.1016/j.talanta.2011.06.021

Carvalho W, Vignado C, Fontana J (2008) Ni(II) removal from aqueous effluents by silylated clays. J Hazard Mater 153:1240–1247. https://doi.org/10.1016/j.jhazmat.2007.09.083

Chen C-Y, Chang T-H, Kuo J-T et al (2008) Characteristics of molybdate-impregnated chitosan beads (MICB) in terms of arsenic removal from water and the application of a MICB-packed column to remove arsenic from wastewater. Bioresour Technol 99:7487–7494. https://doi.org/10.1016/j.biortech.2008.02.015

Chen D, Huang C, He M, Hu B (2009) Separation and preconcentration of inorganic arsenic species in natural water samples with 3-(2-aminoethylamino) propyltrimethoxysilane modified ordered mesoporous silica micro-column and their determination by inductively coupled plasma optical emission spectrometry. J Hazard Mater 164:1146–1151. https://doi.org/10.1016/j.jhazmat.2008.09.022

Chen H, Meshik AP, Pravdivtseva OV et al (2019) Potassium isotope fractionation during high-temperature evaporation determined from the Trinity nuclear test. Chem Geol 522:84–92. https://doi.org/10.1016/j.chemgeo.2019.04.028

Chen X, Wu L, Liu F et al (2018) Performance and mechanisms of thermally treated bentonite for enhanced phosphate removal from wastewater. Environ Sci Pollut Res 25:15980–15989. https://doi.org/10.1007/s11356-018-1794-8

Cortés-Arriagada D, Toro-Labbé A (2016) Aluminum and iron doped graphene for adsorption of methylated arsenic pollutants. Appl Surf Sci 386:84–95. https://doi.org/10.1016/j.apsusc.2016.05.154

Cui H, Qian Y, Li Q et al (2013) Fast removal of Hg(II) ions from aqueous solution by amine-modified attapulgite. Appl Clay Sci 72:84–90. https://doi.org/10.1016/j.clay.2013.01.003

Gohain MB, Pawar RR, Karki S et al (2020) Development of thin film nanocomposite membrane incorporated with mesoporous synthetic hectorite and MSH@UiO-66-NH2 nanoparticles for efficient targeted feeds separation, and antibacterial performance. J Membr Sci 609:118212. https://doi.org/10.1016/j.memsci.2020.118212

Gong X-J, Li W-G, Zhang D-Y et al (2015) Adsorption of arsenic from micro-polluted water by an innovative coal-based mesoporous activated carbon in the presence of co-existing ions. Int Biodeterior Biodegrad 102:256–264. https://doi.org/10.1016/j.ibiod.2015.01.007

Hao J, Han M-J, Wang C, Meng X (2009) Enhanced removal of arsenite from water by a mesoporous hybrid material—Thiol-functionalized silica coated activated alumina. Microporous Mesoporous Mater 124:1–7. https://doi.org/10.1016/j.micromeso.2009.03.021

He H, Tao Q, Zhu J et al (2013) Silylation of clay mineral surfaces. Appl Clay Sci 71:15–20. https://doi.org/10.1016/j.clay.2012.09.028

Karki S, Gohain MB, Yadav D, Ingole PG (2021) Nanocomposite and bio-nanocomposite polymeric materials/membranes development in energy and medical sector: a review. Int J Biol Macromol 193:2121–2139. https://doi.org/10.1016/j.ijbiomac.2021.11.044

Karki S, Ingole PG (2022) Development of polymer-based new high performance thin-film nanocomposite nanofiltration membranes by vapor phase interfacial polymerization for the removal of heavy metal ions. Chem Eng J 446:137303. https://doi.org/10.1016/j.cej.2022.137303

Kecili R, Hussain CH (2018) Mechanism of adsorption on nanomaterials nanomaterials in chromatography. Current Trends in Chromatography Research Technology and Techniques. https://doi.org/10.1016/B978-0-12-812792-6.00004-2

Kumar R, Patel M, Singh P et al (2019) Emerging technologies for arsenic removal from drinking water in rural and peri-urban areas: methods, experience from, and options for Latin America. Sci Total Environ 694:133427. https://doi.org/10.1016/j.scitotenv.2019.07.233

Lalhmunsiama LSM, Tiwari D (2013) Manganese oxide immobilized activated carbons in the remediation of aqueous wastes contaminated with copper(II) and lead(II). Chem Eng J 225:128–137. https://doi.org/10.1016/j.cej.2013.03.083

Lalhmunsiama TD, Lee S-M (2015) Physico-chemical studies in the removal of Sr(II) from aqueous solutions using activated sericite. J Environ Radioact 147:76–84. https://doi.org/10.1016/j.jenvrad.2015.05.017

Lee SM, Lalhmunsiama T, Tiwari D (2015) Porous hybrid materials in the remediation of water contaminated with As(III) and As(V). Chem Eng J 270:496–507. https://doi.org/10.1016/j.cej.2015.02.053

Lee SM, Tiwari D (2012) Organo and inorgano-organo-modified clays in the remediation of aqueous solutions: an overview. Appl Clay Sci 59–60:84–102. https://doi.org/10.1016/j.clay.2012.02.006

Li P, Zhang X, Chen Y et al (2014) One-pot synthesis of thiol- and amine-bifunctionalized mesoporous silica and applications in uptake and speciation of arsenic. RSC Adv 4:49421–49428. https://doi.org/10.1039/C4RA06563H

Li Z, Liu X, Jin W et al (2019) Adsorption behavior of arsenicals on MIL-101(Fe): the role of arsenic chemical structures. J Colloid Interface Sci 554:692–704. https://doi.org/10.1016/j.jcis.2019.07.046

Litter MI, Ingallinella AM, Olmos V et al (2019) Arsenic in Argentina: Technologies for arsenic removal from groundwater sources, investment costs and waste management practices. Sci Total Environ 690:778–789. https://doi.org/10.1016/j.scitotenv.2019.06.358

Luo X, Wang C, Luo S et al (2012) Adsorption of As (III) and As (V) from water using magnetite Fe3O4-reduced graphite oxide–MnO2 nanocomposites. Chem Eng J 187:45–52. https://doi.org/10.1016/j.cej.2012.01.073

Maji S, Ghosh A, Gupta K et al (2018) Efficiency evaluation of arsenic(III) adsorption of novel graphene oxide@iron-aluminium oxide composite for the contaminated water purification. Sep Purif Technol 197:388–400. https://doi.org/10.1016/j.seppur.2018.01.021

Maji SK, Pal A, Pal T (2007) Arsenic removal from aqueous solutions by adsorption on laterite soil. J Environ Sci Health Part A 42:453–462. https://doi.org/10.1080/10934520601187658

Medda N, De SK, Maiti S (2021) Different mechanisms of arsenic related signaling in cellular proliferation, apoptosis and neo-plastic transformation. Ecotoxicol Environ Saf 208:111752. https://doi.org/10.1016/j.ecoenv.2020.111752

Mishra T, Mahato DK (2016) A comparative study on enhanced arsenic(V) and arsenic(III) removal by iron oxide and manganese oxide pillared clays from ground water. J Environ Chem Eng 4:1224–1230. https://doi.org/10.1016/j.jece.2016.01.022

Mohammed AA, Samaka IS (2018) Bentonite coated with magnetite Fe 3 O 4 nanoparticles as a novel adsorbent for copper (II) ions

removal from water/wastewater. Environ Technol Innov 10:162–174. https://doi.org/10.1016/j.eti.2018.02.005
Mohan D, Pittman CU (2007) Arsenic removal from water/wastewater using adsorbents—a critical review. J Hazard Mater 142:1–53. https://doi.org/10.1016/j.jhazmat.2007.01.006
Mostofi Sarkari N, Doğan Ö, Bat E et al (2019) Assessing effects of (3-aminopropyl)trimethoxysilane self-assembled layers on surface characteristics of organosilane-grafted moisture-crosslinked polyethylene substrate: a comparative study between chemical vapor deposition and plasma-facilitated in situ grafting methods. Appl Surf Sci 497:143751. https://doi.org/10.1016/j.apsusc.2019.143751
Najib N, Christodoulatos C (2019) Removal of arsenic using functionalized cellulose nanofibrils from aqueous solutions. J Hazard Mater 367:256–266. https://doi.org/10.1016/j.jhazmat.2018.12.067
Ociński D, Jacukowicz-Sobala I, Mazur P et al (2016) Water treatment residuals containing iron and manganese oxides for arsenic removal from water—characterization of physicochemical properties and adsorption studies. Chem Eng J 294:210–221. https://doi.org/10.1016/j.cej.2016.02.111
Paul B, Martens WN, Frost RL (2011) Organosilane grafted acid-activated beidellite clay for the removal of non-ionic alachlor and anionic imazaquin. Appl Surf Sci 257:5552–5558. https://doi.org/10.1016/j.apsusc.2011.01.034
Prabhu PP, Prabhu B (2018) A review on removal of heavy metal ions from waste water using natural/ modified bentonite. MATEC Web Conf 144:02021. https://doi.org/10.1051/matecconf/201814402021
Qin Z, Yuan P, Yang S et al (2014) Silylation of Al13-intercalated montmorillonite with trimethylchlorosilane and their adsorption for Orange II. Appl Clay Sci 99:229–236. https://doi.org/10.1016/j.clay.2014.06.038
Sabir S, Akash MSH, Fiayyaz F et al (2019) Role of cadmium and arsenic as endocrine disruptors in the metabolism of carbohydrates: inserting the association into perspectives. Biomed Pharmacother 114:108802. https://doi.org/10.1016/j.biopha.2019.108802
Şahan T, Erol F, Yılmaz Ş (2018) Mercury(II) adsorption by a novel adsorbent mercapto-modified bentonite using ICP-OES and use of response surface methodology for optimization. Microchem J 138:360–368. https://doi.org/10.1016/j.microc.2018.01.028
Sarkar A, Paul B (2016) The global menace of arsenic and its conventional remediation—a critical review. Chemosphere 158:37–49. https://doi.org/10.1016/j.chemosphere.2016.05.043
Sarkar B, Xi Y, Megharaj M, Naidu R (2011) Orange II adsorption on palygorskites modified with alkyl trimethylammonium and dialkyl dimethylammonium bromide—an isothermal and kinetic study. Appl Clay Sci 51:370–374. https://doi.org/10.1016/j.clay.2010.11.032
Song P, Yang Z, Zeng G et al (2017) Electrocoagulation treatment of arsenic in wastewaters: a comprehensive review. Chem Eng J 317:707–725. https://doi.org/10.1016/j.cej.2017.02.086
Su J, Lin H, Wang Q-P et al (2011) Adsorption of phenol from aqueous solutions by organomontmorillonite. Desalination 269:163–169. https://doi.org/10.1016/j.desal.2010.10.056
Su L, Tao Q, He H et al (2013) Silylation of montmorillonite surfaces: dependence on solvent nature. J Colloid Interface Sci 391:16–20. https://doi.org/10.1016/j.jcis.2012.08.077
Tcheumi HL, Tonle IK, Ngameni E, Walcarius A (2010) Electrochemical analysis of methylparathion pesticide by a gemini surfactant-intercalated clay-modified electrode. Talanta 81:972–979. https://doi.org/10.1016/j.talanta.2010.01.049
Te B (2017) Adsorptive behavior of low-cost modified natural clay adsorbents for arsenate removal from water. Int J Geomate. https://doi.org/10.21660/2017.33.2531
Thanhmingliana TD (2015) Efficient use of hybrid materials in the remediation of aquatic environment contaminated with micropollutant diclofenac sodium. Chem Eng J 263:364–373. https://doi.org/10.1016/j.cej.2014.10.102
Tiwari D, Lee SM (2012) Novel hybrid materials in the remediation of ground waters contaminated with As (III) and As (V). Chem Eng J 204:23–31
Tonlé IK, Diaco T, Ngameni E, Detellier C (2007) Nanohybrid Kaolinite-based materials obtained from the interlayer grafting of 3-Aminopropyltriethoxysilane and their potential use as electrochemical sensors. Chem Mater 19:6629–6636. https://doi.org/10.1021/cm702206z
Tonlé IK, Ngameni E, Tcheumi HL et al (2008) Sorption of methylene blue on an organoclay bearing thiol groups and application to electrochemical sensing of the dye. Talanta 74:489–497. https://doi.org/10.1016/j.talanta.2007.06.006
Undabeytia T, Madrid F, Vázquez J, Pérez-Martínez JI (2019) Grafted Sepiolites for the removal of pharmaceuticals in water treatment. Clays Clay Miner 67:173–182. https://doi.org/10.1007/s42860-019-00013-4
Uppal JS, Zheng Q, Le XC (2019) Arsenic in drinking water—recent examples and updates from Southeast Asia. Curr Opin Environ Sci Health 7:126–135. https://doi.org/10.1016/j.coesh.2019.01.004
Vahedi A, Rahmani M, Rahmani Z et al (2018) Application of polymer-sepiolite composites for adsorption of Cu(II) and Ni(II) from aqueous solution: equilibrium and kinetic studies. E-Polym 18:217–228. https://doi.org/10.1515/epoly-2017-0170
Wamba AGN, Kofa GP, Koungou SN et al (2018) Grafting of Amine functional group on silicate based material as adsorbent for water purification: a short review. J Environ Chem Eng 6:3192–3203. https://doi.org/10.1016/j.jece.2018.04.062
Wang C, Luan J, Wu C (2019) Metal-organic frameworks for aquatic arsenic removal. Water Res 158:370–382. https://doi.org/10.1016/j.watres.2019.04.043
WHO (2011) WHO: Guidelines for drinking-water quality-Google Scholar. https://scholar.google.com/scholar_lookup?title=Arsenic%20in%20Drinking-Water.%20Background%20Document%20for%20Preparation%20of%20WHO%20Guidelines%20for%20Drinking-water%20Quality&author=WHO&publication_year=2003. Accessed 31 May 2021
Yadav MK, Saidulu D, Gupta AK et al (2021) Status and management of arsenic pollution in groundwater: a comprehensive appraisal of recent global scenario, human health impacts, sustainable field-scale treatment technologies. J Environ Chem Eng 9:105203. https://doi.org/10.1016/j.jece.2021.105203

Yin H, Kong M, Gu X, Chen H (2017) Removal of arsenic from water by porous charred granulated attapulgite-supported hydrated iron oxide in bath and column modes. J Clean Prod 166:88–97. https://doi.org/10.1016/j.jclepro.2017.08.026

Yılmaz Ş, Şahan T, Karabakan A (2017) Response surface approach for optimization of Hg(II) adsorption by 3-mercaptopropyl trimethoxysilane-modified kaolin minerals from aqueous solution. Korean J Chem Eng 34:2225–2235. https://doi.org/10.1007/s11814-017-0116-z

Zhang J, Ding T, Zhang Z et al (2015) Enhanced adsorption of trivalent arsenic from water by functionalized diatom silica shells. PLoS ONE 10:e0123395. https://doi.org/10.1371/journal.pone.0123395

Zhu N, Yan T, Qiao J, Cao H (2016a) Adsorption of arsenic, phosphorus and chromium by bismuth impregnated biochar: adsorption mechanism and depleted adsorbent utilization. Chemosphere 164:32–40. https://doi.org/10.1016/j.chemosphere.2016.08.036

Zhu R, Chen Q, Zhou Q et al (2016b) Adsorbents based on montmorillonite for contaminant removal from water: a review. Appl Clay Sci 123:239–258. https://doi.org/10.1016/j.clay.2015.12.024